Chapter 9

Exotic Electrostatics: Unusual Features of Electrostatic Interactions between Macroions

Ali Naji
Department of Applied Mathematics and Theoretical Physics, University of Cambridge, Cambridge CB3 0WA, United Kingdom

Matej Kanduč
Department of Theoretical Physics, J. Stefan Institute, SI-1000 Ljubljana, Slovenia

Roland R. Netz
Department of Physics, Technical University of Munich, James Franck Strasse, D-85748 Garching, Germany

Rudolf Podgornik
Department of Theoretical Physics, J. Stefan Institute, SI-1000 Ljubljana, Slovenia
and
Department of Physics, Faculty of Mathematics and Physics and Institute of Biophysics, Medical Faculty, University of Ljubljana, SI-1000 Ljubljana, Slovenia

We present an overview of our understanding of electrostatic interactions between charged macromolecular surfaces mediated by mobile counter- and coions. The dichotomy between the *weak* and the *strong coupling* regimes is described in detail and the way they engender repulsive and attractive interactions between nominally equally charged macroions. We also introduce the concept of *dressed counterions* in the case of many-component Coulomb fluids that are partially weakly and partially strongly coupled to local electrostatic fields leading to non-monotonic interactions between equally charged macroions. The effect of quenched surface charge disorder on the counterion-mediated electrostatic interactions is analyzed within the same conceptual framework and shown to

lead to unexpected and extraordinary electrostatic interactions between randomly charged surfaces with equal mean surface charge densities or even between effectively neutral macroion surfaces. As a result, these recent developments challenge some cherished notions of pop culture.

1. Introduction

The nature of electrostatic interactions between charges started to be studied intensively in the second half of the 18th century.[1] Benjamin Franklin first inferred from an observation that surprisingly there is no force on a charge inside a charged sphere, an observation later repeated by Joseph Priestley (1767). John Robison (1769) determined that the electrostatic force falls off with (almost) the second power of separation between charges. Based on the work of Charles A. de Coulomb (1777) who is a co-inventor of the torsion balance for measuring the force of magnetic and electrical attraction, Henry Cavendish measured directly the interactions between charges (1779) but did not publish his results. They were eventually published by William Thomson (Lord Kelvin) one hundred years after the original discovery (1879). From hard science electrostatic interaction penetrated the pop culture in general and today everybody knows that *opposites attract* and *likes repel!*

The exact form of the electrostatic interaction is since known to be given by the Coulomb's law which states that the interaction potential between two charges e_1 and e_2 *in vacuo* located at $\mathbf{r}$ and $\mathbf{r}'$ respectively, can be written in the standard form (in SI units) as

$$V(\mathbf{r},\mathbf{r}') = \frac{e_1 e_2}{4\pi\varepsilon_0|\mathbf{r}-\mathbf{r}'|}, \tag{1}$$

were ε_0 is the permittivity of vacuum. Electrostatic interaction is the fundamental interaction in molecular world giving rise to short range intramolecular bonds as well as longer ranged interactions between molecules and their aggregates.[2] While atomic bonds are obtained by combining the Coulomb potential with the quantum of action, longer ranged colloidal and nanoscale electrostatic interactions are obtained by combining the Coulomb potential with the thermal energy $k_{\rm B}T$.

Almost exactly a hundred years ago Gouy[3] and Chapman[4] were the first to combine thermal energy and Coulomb interactions into a statistical theory of Coulomb fluids basing their approach on what became later known as the *Poisson-Boltzmann (PB) equation*. *Coulomb fluid* in general is an assembly of (variously) charged particles in thermal equilibrium. This

mean-field approach to Coulomb fluids was gradually elaborated in uncountably many ways starting from the seminal work of Debye and Hückel[5] and finally codified as a cornerstone of the fundamental DLVO theory of colloidal interactions by Derjaguin and Landau[6] as well as Verwey and Overbeek,[7] where it figures as the repulsive electrostatic part of the total disjoining pressure acting between macromolecular bodies.[8,9] The attractive component in this case is provided solely by the van der Waals interactions that have their origin in the quantum and thermal fluctuations of electromagnetic fields.[10]

One could claim that modern formulation of statistical mechanics of Coulomb fluids starts with the work of Edwards and Lenard[11] where the grand-canonical partition function of a Coulomb fluid was written in the form of a functional integral over fluctuating electrostatic fields. While Podgornik and Žekš[12] realized that the collective description based on the mean-field PB theory arises from the *saddle-point approximation* to this functional integral in the case of a *weak coupling regime* corresponding, for instance, to small external charges, Netz showed[13,14] that another approximation valid in the regime of large external charges leads to a completely different fixed point, formulated in terms of a single-particle description of the same system. This so-called *strong coupling regime* has been the focus of various theoretical studies over the past decade.[15–19] The two approximations were shown to correspond to extremal values of a single electrostatic coupling parameter and to consistently bracket all available simulation results on statistical properties of non-homogeneous Coulomb fluids,[15,16] i.e., Coulomb fluids confined between charged boundaries.

In what follows we shall describe the main consequences of this *weak-strong coupling dichotomy* especially as they transpire in the case of interactions between charged (planar) macromolecular surfaces across a Coulomb fluid comprising mobile counter- and coions. We shall see that the counterion-mediated electrostatic interactions are strictly repulsive in symmetric external charge configurations for the case of weak coupling but can turn attractive for strongly coupled surfaces. In the case of many-component systems, composed typically of a weakly coupled univalent salt and strongly coupled polyvalent counterions, these interactions show a subtle interplay between repulsions and attractions for nominally equally charged surfaces. On the other hand, the presence of quenched charge disorder on bounding surfaces can lead to pronounced electrostatic attraction. These exotic features only arise in special cases of strongly coupled systems and can not be rationalized within the standard mean-field PB approach.

2. Scenery

Electric charges and electrostatic interactions are ubiquitous in soft-matter and biological systems.[20,21] *Soft materials* are typically composed of *macromolecules* such as polymers, colloids and proteins which often acquire surface charges when dissolved in a polar solvent like water. This is usually due to dissociation of surface chemical groups, which leaves permanent charges on macromolecular surfaces and releases oppositely charged microscopic *counterions* into the solution. Soft materials are easily deformed or re-arranged by interaction potentials comparable in magnitude to thermal energy. It thus becomes clear that electrostatic interactions, that are typically long-ranged and strong, constitute a prominent factor in determining the behavior and properties of soft materials. This makes charged materials central to many technological applications and on the other hand, a challenging subject for fundamental research in inter-disciplinary sciences.[2] In what follows, we briefly review a few examples to demonstrate the diversity of phenomena associated with charged soft-matter systems.

2.1. *Colloids, polymers and membranes: The mesoscopic scale*

Colloids are abundant in nature and industry: smoke, fog, milk, paint and ink are only a few examples of colloidal systems. They comprise tiny solid or liquid particles that are suspended in another medium such as air or another liquid. An important factor, which makes colloidal solutions in many ways different from molecular or simple electrolyte solutions (such as sugar or salt solution), is the large asymmetry in size and mass between the colloidal particles and solvent molecules (or microscopic ions): colloids are *mesoscopic* or even *nanoscopic* particles with sizes in the range of a few nanometers to microns that are indeed made of many atoms, but not yet sufficiently many to make them behave like macroscopic bodies.

In colloidal dispersions, the total area that is in contact with solvent is tremendously large: for nanometer-sized colloids, nearly half of the atoms are at the surface whereas for macroscopic bodies this ratio tends to zero. This is even more true for extended quasi-two-dimensional macromolecular aggregates such as lipid membranes and surfactant-covered interfaces that can carry a substantial amount of charged molecular moieties.[21] Therefore, contrary to the typical situation in the macroscopic world, the physics of meso- and nanoscopic particles are dominated by "surface" properties and interactions.[7–9]

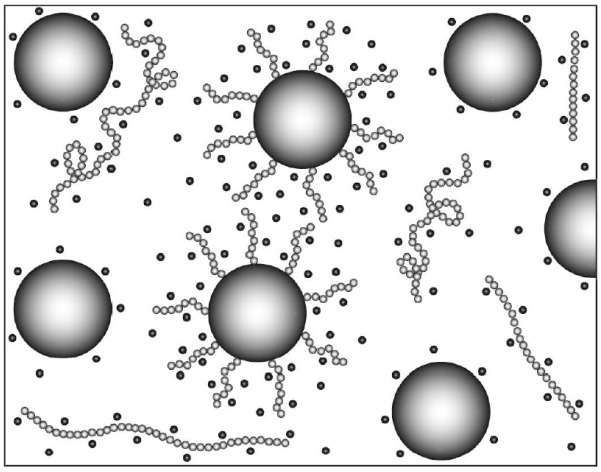

Fig. 1. Schematic view of a charged solution consisting of charged colloids (dark spheres), charged polymer chains and microscopic neutralizing counterions (small black spheres). Colloids may be covered by charged polymer brushes, which generate an additional repulsive interaction between them.

Another relevant mesoscopic or *macromolecular* system are polymers (with everyday-life examples like chewing gum, dough or egg white), in which many repeating subunits (monomers) are chemically connected to form a flexible chain. Flexible polymers are distinguished by their many degrees of freedom associated with conformational rearrangements of monomers that are easily excited by thermal energy at room temperature leading to a diverse phase behavior spanning extended and strongly entangled polymers such as DNA in solution, all the way to collapsed polymer chains organizing into compact globular states as in the case of proteins. Depending on their chemical structure, polymer chains can have a large mechanical stiffness as well, behaving like rigid rods at small length scales, or can be substantially charged giving rise to *polyelectrolytes*, in both cases playing an important role in biological processes occurring in the cell.[22]

2.2. *Charges: from industry to biology*

In the mesoscopic world, only electromagnetic interactions that emerge in a variety of forms, are important; they are capable of overcoming thermal fluctuations–which are characterized by an energy scale of about $0.025e$V at room temperature[8]–and thus enable formation of stable *condensed* phases for soft complex materials.

In general, colloids dissolved in an aqueous solvent attract each other due to ubiquitous van der Waals dispersion forces that result from induced charges on their surface.[2] As a result, colloidal particles tend to form large aggregates that typically sediment and destroy the dispersion. In many applications (for example in food emulsions such as milk), however, stability of a colloidal dispersion is a desirable property. One way to stabilize dispersions against aggregation is to generate long-range repulsive interactions between colloidal particles by charging their surfaces, which leads to the DLVO mechanism for the stability of colloidal dispersions.[6,7] Another method of stabilization is to end-graft polymer chains (or *polymer brushes*) to the particle surfaces.[23] For this task, charged polymers are ideal since they swell substantially in aqueous solutions and inhibit close contact between colloids (see Fig. 1). This latter mechanism has the advantage that it is highly stable against the addition of electrolyte or salt ions.[24]

Charged polymers, or *polyelectrolytes*, play a significant role in the production of cheap, non-toxic and environmentally friendly materials.[25,26] In contrast to water-insoluble hydrocarbon chains, polyelectrolytes typically show high affinity for water and heavy metal ions, which makes them useful in applications such as super-absorbing diapers, waste water purifiers and washing detergents and their additives.

In biology electrostatic effects between charged polymers such as DNA and RNA are ubiquitous.[20] DNA, for instance, is a long biomolecule with a total length of about two meters in human cells, bearing one elementary charge per 1.7Å, which for human DNA adds up to 10^{10} elementary charges overall! Yet the DNA is densely packed inside the cell nucleus with a diameter of less than a few microns. In eucaryotic cells, this storage process involves a hierarchical structure on the lowest level of which short segments of DNA are tightly wrapped around positively charged histone protein complexes of a few nanometers in diameter.[22] This protein-DNA complexation is believed to be governed by electrostatic interactions.[15,27,28] Electrostatic effects also play a key role in complexes of DNA with cationic lipids,[29–31] which are promising synthetically based non-viral carriers of DNA for gene therapy.[32]

Another example (which is closely related to the results presented later in this chapter) is the DNA condensation,[20,33,34] in which electrostatic effects enter in a counter-intuitive fashion: here like-charged segments of DNA strongly attract each other! In the *in vitro* experiments,[35] the condensation of DNA is realized using bacteriophages, which consist of a rigid

shell (the capsid) that accommodates a single molecule of viral DNA. These viruses can inject their DNA into a cell or a lipid vesicle. As a result, large lengths of DNA (up to a hundred microns) can be fitted and condensed into a tightly packed, circumferentially wound torus with a diameter of about a hundred nanometers. This packaging process, which works against the Coulomb self-repulsion and the conformational entropy of the DNA chain, is facilitated and depends upon the presence of high-valency counterions in the medium. Similarly, other highly charged polymers, such as negatively charged F-actin and microtubules can aggregate into closely packed rod-like bundles when small amounts of polyvalent cations are added to the solution.[36–38] It turns out that, in general, when particles are strongly charged, the role of electrostatic interactions dramatically changes:[15] here electrostatic interactions themselves can trigger the destabilization of charged solutions by mediating attractive like-charge interactions!

2.3. *Theoretical challenge and coarse-grained models*

From a theoretical point of view, charged systems pose a many-body problem: *macroions*, such as charged colloids and polymers, and other charged macromolecular surfaces, such as lipid membranes and surfactant layers, are always surrounded by counterions, and also in general by coions. These particles form loosely bound ionic clouds around macroions and tend to screen their charges. In particular, counterions that are attracted towards macromolecular surfaces, predominantly determine the static and dynamic properties of macromolecular solutions. Understanding the interactions between macromolecules across an ionic medium thus requires an understanding of the counterionic clouds first.

In the most common theoretical approaches known also as *primitive models*, the molecular nature of the solvent is neglected and is represented by a continuum dielectric medium. In reality, the solvent structure is locally perturbed around particles, which can give rise to additional short-ranged solvent-induced interactions.[8,39,40] On the other hand, the microscopic features of the macroions are taken into account using coarse-grained models that incorporate only a few effective parameters such as an effective surface charge density. In most cases, the specific effects associated with ions[39] as well as the image charge effects due to dielectric inhomogeneities are also neglected. These models therefore represent a *crude simplification* of reality, yet given those simplifications, they can still lead to a systematic and clear understanding of electrostatic effects.

Here we shall first begin by adopting such a simple model for the interaction between charged macromolecular surfaces in the presence of *counterions only*, but then examine the effects due to the additional salt[41] and the heterogeneous or *disordered* distribution of surface charges[42–45] in more detail. For simplicity, we shall also focus only on the case of *planar* charged surfaces, appropriate for the case of charged membranes, solid substrates, or large colloids. Other factors such as non-planar geometry of charged surfaces,[46–48] image charges,[43,48–50] dissimilar surfaces[51] or multipolar structure of counterions[52] have been analyzed within the same context.

3. Length Scales in a Classical Charged System

Consider a system of fixed charged objects with uniform surface charge density $-\sigma_{\rm s}e_0$ (with e_0 being the elementary charge) that are surrounded by their neutralizing counterions of charge valency $+q$ in a solvent of dielectric constant ε at temperature T.[a]

One of the basic characteristic length scales in a charged system is the *Bjerrum length*[53]

$$\ell_{\rm B} = e_0^2/(4\pi\varepsilon\varepsilon_0 k_{\rm B}T), \tag{2}$$

which is set by the ratio between the thermal energy, $k_{\rm B}T$, and the Coulomb interaction energy between two elementary charges at separation r, i.e., $V/(k_{\rm B}T) = \ell_{\rm B}/r$. The Bjerrum length thus measures the distance at which two elementary charges interact with an energy equal to $k_{\rm B}T$. In water and at room temperature ($\varepsilon = 80$), one has $\ell_{\rm B} \simeq 7.1$Å. For counterions of charge valency $+q$, the Bjerrum length may be redefined as $q^2\ell_{\rm B}$.

Other length scales may be identified by considering the specific form of the charge distribution and geometry of macroions. For uniformly charged planar surfaces (Fig. 2), one can define another key length scale by comparing the thermal energy with the energy scale of the counterion-wall attraction, i.e., $u/(k_{\rm B}T) = z/\mu$, where z is the distance from the wall and

$$\mu = 1/(2\pi q\ell_{\rm B}\sigma_{\rm s}) \tag{3}$$

is known as the *Gouy-Chapman (GC) length*.[3,4] The GC length measures the distance at which the thermal energy equals the counterion-wall electrostatic interaction energy. It also gives a measure of the *thickness* of the counterion layer at a charged wall as we shall see later.

[a]We conventionally assume that macroions are negatively charged and counterions are positively charged, thus $\sigma_{\rm s}$ and q are both positive by definition.

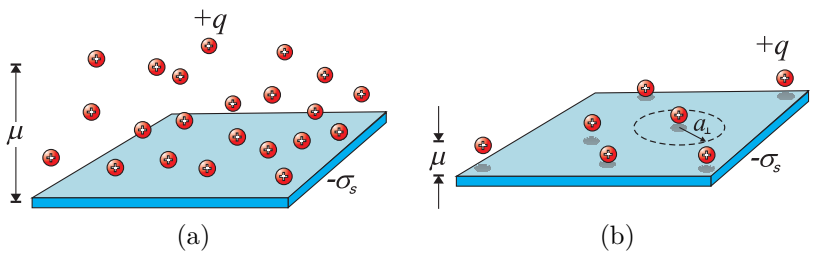

Fig. 2. Schematic view of the structure of a layer of counterions at an oppositely charged surface for small (a) and large (b) value of the coupling parameter.

For planar systems where no other length scales are present, it follows that only the dimensionless ratio between the above two length scales matters, i.e.,

$$\Xi = q^2 \ell_{\rm B}/\mu = 2\pi q^3 \ell_{\rm B}^2 \sigma_{\rm s}. \tag{4}$$

This parameter is known as the *electrostatic coupling parameter*.[13,14]

4. From Mean-Field to Strong Coupling Regime

For small coupling parameters $\Xi \ll 1$, equation (4) shows that the GC length is relatively large, which indicates that counterions form a loosely bound cloud at an oppositely charged wall (Fig. 2(a)). For large coupling parameter $\Xi \gg 1$, in contrast, the GC length is relatively small and counterions are strongly attracted toward the wall (Fig. 2(b)). Further insight may be obtained by considering the typical distance between counterions at a charged surface. For counterions residing near the surface, the local electroneutrality condition implies a typical lateral separation of

$$a_\perp \sim \sqrt{q/\sigma_{\rm s}}, \tag{5}$$

since each counterion neutralizes the charge of an area that scales as $a_\perp^2 \sim q/\sigma_{\rm s}$. Counterion spacing $a_\perp$ is not an independent length scale and may be written in the units of the GC length as

$$(a_\perp/\mu) \sim \sqrt{\Xi}. \tag{6}$$

4.1. *Weak coupling or mean-field regime*

In the regime where $\Xi \ll 1$, equation (6) shows that the lateral separation of counterions near the surface is small compared with the typical layer

thickness, μ, which further indicates that the counterions tend to form a diffuse fluid-like layer at the surface (Fig. 2(a)).[b] This regime is dominated by collective mean-field-like effects, i.e., counterions become uncorrelated from each other in a statistical sense as each counterion in the layer interacts with a diffuse cloud of many other counterions. Therefore, $\Xi \ll 1$ identifies the *weak coupling* (WC) or *mean-field regime*, which is relevant to systems with weakly charged surfaces, low valency counterions and/or high temperature.[15]

Formally, one can employ a mean-field approximation in order to describe the system in the WC regime by neglecting all inter-particle correlations on the leading order. The mean-field approximation is exact in the limit $\Xi \to 0$[54] and leads to the so-called Poisson-Boltzmann (PB) equation for the mean-field electrostatic potential $\psi(\mathbf{r})$,[7,8] i.e.

$$-\varepsilon\varepsilon_0\nabla^2\psi = \rho_0(\mathbf{r}) + qe_0n_0\,\Omega(\mathbf{r})\,\exp(-\beta qe_0\psi), \tag{7}$$

where $\beta = 1/(k_{\rm B}T)$. The first term on the r.h.s. represents the charge distribution due to fixed external charges (macroions), $\rho_0(\mathbf{r})$, and the second term is the mean-field number density of counterions $n_{\rm PB}(\mathbf{r}) = n_0\,\Omega(\mathbf{r})\,\exp(-\beta qe_0\psi)$, where n_0 is a normalization prefactor. The "blip" function $\Omega(\mathbf{r})$ is equal to one in the region accessible to counterions and zero elsewhere.

For point-like counterions at a single uniformly charged wall, the PB equation yields the well-known algebraically decaying density profile[7,8]

$$\frac{n_{\rm PB}(z)}{2\pi\ell_{\rm B}\sigma_{\rm s}^2} = \frac{1}{(z/\mu+1)^2} \qquad z>0, \tag{8}$$

where z is the distance from the wall. Note that the density profile is normalizable to the total number of counterions in order to ensure electroneutrality, and that the GC length, μ, equals the height of a layer containing *half* of the counterions, thus giving a measure of the typical layer thickness. The *contact* density of counterions $n_{\rm PB}(z=0) = 2\pi\ell_{\rm B}\sigma_{\rm s}^2$ turns out to be an exact result within the present model and remains valid beyond the mean-field theory.[55]

4.2. *Strong coupling regime*

In the *strong coupling (SC) regime* $\Xi \gg 1$, equation (6) shows that the lateral separation of counterions becomes larger than the GC length, thus

[b] A more accurate estimate of the typical distance, a, between counterions in an extended three-dimensional layer gives $a/\mu \sim \Xi^{1/3}$.[13]

indicating that the counterions tend to form a quasi-2D layer at the surface (Fig. 2(b)). Such a layer is dominated by strong mutual repulsions between counterions as can be seen by considering the effective 2D plasma parameter[56] $\Gamma \equiv q^2\ell_{\rm B}/a_\perp \sim \Xi^{1/2}$, which gives the ratio between Coulombic inter-particle repulsions and the thermal energy. For elevated Ξ, Coulombic repulsions tend to freeze out lateral fluctuations of counterions on the surface, leading to *strong correlations* and a trend toward crystallization in the ionic structure.[17,18] Individual counterions thus become isolated in relatively large *correlation holes* of size $a_\perp$ from which neighboring counterions are statistically depleted. The Wigner crystallization of the 2D one-component plasma is known to occur for $\Gamma > \Gamma_c \simeq 125$,[56] which corresponds to the range of coupling parameters $\Xi > \Xi_c \simeq 3.1 \times 10^4$.[14]

For $\Xi \gg 1$, the PB description completely breaks down, nonetheless, one can obtain a simple analytical theory by employing a virial and $1/\Xi$ expansion to the leading order, which is known as the *strong coupling theory*.[13] The SC theory turns out to contain contributions that involve only single-particle interaction energies between counterions and the fixed macroion surface charges. For instance, the SC density profile of counterions at a single charged wall comes exclusively from the vertical degree of freedom, z, through which single isolated counterions are coupled to the wall with the interaction potential $u/(k_{\rm B}T) = z/\mu$. Hence using the Boltzmann weight, one finds the (laterally averaged) density profile

$$n_{\rm SC}(z) = n_0 \exp(-z/\mu), \tag{9}$$

where the prefactor (contact density) is again found from the electroneutrality condition to be $n_0 = 2\pi\ell_{\rm B}\sigma_{\rm s}^2$. Unlike in the WC case, the SC density profile decays exponentially away from the charged wall. Moreover, the average distance of counterions is finite and equal to the GC length, $\langle z\rangle_{\rm SC} = \mu$, reflecting again the quasi-2D structure of the layer.

Formally, the single-particle SC theory is exact in the asymptotic limit of an infinitely large correlation hole size, $a_\perp/\mu \to \infty$, or simply $\Xi \to \infty$. However, its validity holds in a wider range of system parameters as is evident from comparison with computer simulations.[13,14] For instance, for a *finite* coupling parameter Ξ, the SC density profile (9) still holds approximately at distances $z < a_\perp$, which yields the criterion

$$z/\mu < \sqrt{\Xi}, \tag{10}$$

identifying the limits of applicability of the SC theory. At larger distances $z > a_\perp$, multi-particle interactions become increasingly more important and the mean-field-like features eventually dominate for $z \gg a_\perp$.[13,14]

Table 1. Typical values of physical parameters for some realistic systems.

	σ_s (e_0/nm^2)	q	μ(Å)	Ξ
charged membranes	~ 1	1	2.2	3.1
		2	1.1	24.8
		3	0.7	83.7
DNA	0.9	1 (Na^+)	2.4	2.8
		2 (Mn^{2+})	1.2	22.4
		3 (spd^{3+})	0.8	75.6
		4 (sp^{4+})	0.6	179
highly charged colloids (surfactant micelles)	~ 1	3	0.7	85
weakly charged colloids (polystyrene particles)	~ 0.1	1	~ 2	~ 0.1

In brief, thus, one can identify two asymptotic regimes of weak and strong coupling based on the value of the electrostatic coupling parameter, where a charged system may be studied by means of two limiting theories, namely, the WC (mean-field) and the SC theory.

In Table 1, we present illustrative examples of the parameter values (surface charge density σ_s, counterion valency q, GC length μ, and the coupling parameter Ξ in water and at room temperature) from a few realistic weakly and strongly coupled systems. Note that a typical coupling strength of $\Xi \sim 10^2$ (or larger) already falls within the SC regime and a value of $\Xi \sim 1$ (or smaller) typically well inside the WC regime.[13–16]

5. Interactions between Like-Charged Surfaces

Macroions in solution are often like-charged and thus repel each other by their bare Coulomb interaction. The overall interaction is however different from this bare interaction due to the presence of counterions, which can mediate both *repulsive* and *attractive* effective forces. Obviously, the counterion-mediated interactions depend strongly on the distribution of counterions around macroions.

In order to demonstrate the underlying physical picture, we shall focus on the interaction between two *identical* planar like-charged walls of uniform surface charge density $-\sigma_s e_0$ at separation D, where q-valent counterions fill only the space between the walls, Fig. 3 (the dielectric constant is assumed to be uniform in space). In this system, an extra length scale is set by the wall separation, D. Two limiting regimes of repulsion and attraction may

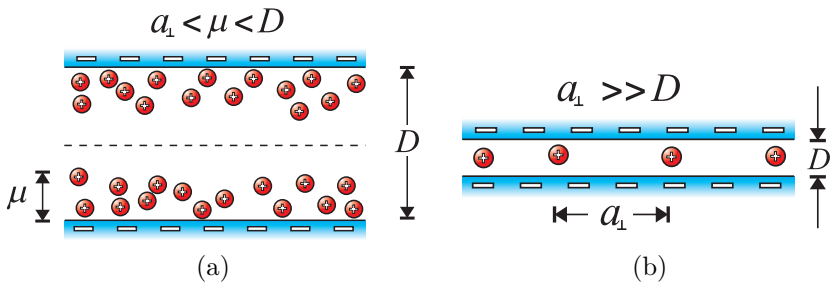

Fig. 3. Schematic representation of the WC (a) and SC (b) interaction regimes for two like-charged walls.

be distinguished qualitatively by comparing D with other length scales of the system as follows.

5.1. *WC regime: Repulsion*

Let us first consider the WC limit, $\Xi \ll 1$, in the regime where the wall separation, D, is large compared with all other length scales (Fig. 3(a)). In this case, counterions form a diffuse layer at each wall, but due to the large separation, the system is approximately decoupled into two nearly neutral sub-systems, each consisting of a charged wall and its counterion cloud. The effective pressure acting between the walls is dominated by the osmotic pressure of counterions across the mid-plane, which is positive and thus corresponds to an effective *repulsion* between the walls. The scaling behavior of this effective repulsion follows by noting that the mid-plane osmotic pressure can be estimated from the local counterion density, $n_{\rm mid}$, and by using the ideal-gas equation of state as $\beta P \sim n_{\rm mid}$. Thus, according to Eq. (8), the interaction pressure is expected to decay as $\sim D^{-2}$.

It turns out that the PB pressure obtained in the limit $\Xi \to 0$ coincides *exactly* with the mid-plane osmotic pressure of counterions as discussed above and may be expressed as[7,8,13]

$$\frac{\beta P_{\rm PB}(D)}{2\pi \ell_{\rm B} \sigma_{\rm s}^2} = \Lambda, \tag{11}$$

where Λ is obtained from $\Lambda^{1/2} \tan[\Lambda^{1/2}(D/2\mu)] = 1$. From here one can obtain the large-separation $D/\mu \gg 1$ behavior

$$\frac{\beta P_{\rm PB}(D)}{2\pi \ell_{\rm B} \sigma_{\rm s}^2} \simeq \left(\frac{\pi \mu}{D}\right)^2. \tag{12}$$

5.2. *SC regime: Attraction*

Now let us consider the SC limit, $\Xi \gg 1$, in the regime where D is smaller than the lateral spacing between counterion, $a_\perp \gg D$ (Fig. 3(b)). Since counterions are highly separated from each other, the two opposite layers of counterions tend to form an inter-locking pattern at small separations.

The system may be thought of as a collection of laterally frozen "correlation cells", each consisting of a single counterion sandwiched between two opposing sections of the walls with lateral size of about $a_\perp$. Since $a_\perp \gg D$, the effective pressure between the walls is dominated by the contribution from single counterions fluctuating in single correlation cells. The electrostatic energy of the system per cell is the sum of the bare interactions between the two surfaces with each other and with the single counterion, which–using the electroneutrality condition per cell and the fact that the wall separation is small–follows as $u_{\rm elec}/(k_{\rm B}T) \simeq 2\pi\ell_{\rm B}\sigma_{\rm s}^2 D$ per unit area. This *energetic* contribution gives an attractive pressure as $\beta P_{\rm elec} \simeq -2\pi\ell_{\rm B}\sigma_{\rm s}^2$ between the walls. On the other hand, the entropic contribution due to counterion confinement is of the order $S_{\rm ci} \sim k_{\rm B} \ln D$ (per cell), which generates a repulsive component. The total pressure between strongly coupled walls is then obtained by combining these two effects as

$$\frac{\beta P_{\rm SC}(D)}{2\pi\ell_{\rm B}\sigma_{\rm s}^2} = -1 + \frac{2\mu}{D}. \tag{13}$$

This expression clearly predicts a closely packed *bound state* for the like-charged walls with an equilibrium surface-surface separation, D^*, equal to twice the GC length, i.e., $D^* = 2\mu$. The like-charged walls therefore *attract* each other for $D > D^*$ and *repel* at smaller separations.

The analytical expression (13) is indeed an exact result for planar walls in the limit $\Xi \to \infty$.[13,14] It turns out that in a system with *finite* coupling parameter, Ξ, the asymptotic ($\Xi \to \infty$) SC results still hold approximately as long as the surface separation, D, is smaller than the typical lateral distance between counterions, $a_\perp$, i.e., for $D < a_\perp$. This condition in fact yields a simple and generic criterion identifying the regime where the SC attraction is expected to emerge between two like-charged macroions. It was originally suggested by Rouzina and Bloomfield[17] and verified and generalized later using extensive analytical and numerical methods.[13–16,41,46–49,51] For larger inter-surface separations, $D > a_\perp$, the mean-field features become increasingly more important and the strength of attraction reduces. Eventually at very large D, the interaction becomes repulsive.[13,14]

6. Counterions with Salt

The SC theory was so far designed exclusively for counterions-only systems, i.e., Coulomb fluids composed of only counterions in the absence of any salt ions.[13] Though an approximation of this type can be used to describe situations where a large amount of polyvalent counterions dominate the system, it has to be amended in the general case in order to deal with the complexity of real systems that always contain some amounts of simple salt.[8] An experimentally oft-encountered situation would be a system composed of fixed surface charges with polyvalent counterions bathed in a solution of univalent salt.[57,58]

This situation leads to a difficult problem of *asymmetric* aqueous electrolytes where different components of the Coulomb fluid are differently coupled to local electrostatic fields.[59] Polyvalent counterions are coupled strongly, whereas univalent salt ions are coupled weakly. In this case no single approximation scheme that would treat all the charged components on the same level would be expected to work. Whereas the SC framework would certainly work for the polyvalent counterions, it would fail for the univalent salt. The converse is true for the WC framework. One is thus faced with a problem since no single approximation scheme appears to be valid in any range of coupling parameters. One can nevertheless build a theoretical framework that allows to *selectively* use different approximation schemes for different components of the asymmetric Coulomb fluid. This combined WC-SC approach appears to bring forth all the salient features of these asymmetric systems at high electrostatic couplings.[41]

6.1. *Functional integral formalism*

Our arguments until now were strictly intuitive. A formal theory can be developed exactly in terms of the functional integral representation of the classical partition function of the Coulomb fluid along the lines first introduced by Edwards and Lenard.[11–13]

Assume first that the system is composed of charged macromolecules with fixed charge density $\rho_0(\mathbf{r})$, mobile polyvalent counterions and an additional univalent salt. The total electrostatic interaction energy of a given configuration of the system can be written as

$$W = \frac{1}{2}\int \rho(\mathbf{r}) v(\mathbf{r},\mathbf{r}') \rho(\mathbf{r}')\, \mathrm{d}\mathbf{r}\, \mathrm{d}\mathbf{r}', \tag{14}$$

where $v(\mathbf{r},\mathbf{r}')$ is the Coulomb kernel given by $v(\mathbf{r},\mathbf{r}')=1/(4\pi\varepsilon\varepsilon_0|\mathbf{r}-\mathbf{r}'|)$, and $\rho(\mathbf{r})$ is the total charge density

$$\rho(\mathbf{r})=\rho_0(\mathbf{r})+\sum_i qe_0\delta(\mathbf{R}_i^c-\mathbf{r})+\sum_i e_0\delta(\mathbf{R}_i^+-\mathbf{r})-\sum_i e_0\delta(\mathbf{R}_i^--\mathbf{r}), \quad (15)$$

where $\mathbf{R}_i^c$, $\mathbf{R}_i^+$ and $\mathbf{R}_i^-$ are the positions of the polyvalent counterions, univalent cations (salt counterions) and univalent anions (salt coions), respectively.[c] Assuming again that the system is composed of two apposed planar surfaces at $z=\pm D/2$ with the surface charge density $-\sigma_{\rm s}$, we have

$$\rho_0(\mathbf{r})=-\sigma_{\rm s}e_0\big[\delta(z-D/2)+\delta(z+D/2)\big]. \quad (16)$$

The salt ions are assumed to be present in all regions in space, whereas the counterions are assumed to be present only in the inter-surface region $|z|<D/2$ as specified by the geometry "blip" function $\Omega(\mathbf{r})$ (Section 4.1).

We then follow the standard procedure by introducing a fluctuating local potential, ϕ, via the Hubbard-Stratonovich transformation, which leads to the following exact functional integral representation for the grand-canonical partition function[12,13]

$$\mathcal{Z}=\int\mathcal{D}\phi\,\mathrm{e}^{-\beta H[\phi]}, \quad (17)$$

where the field-functional Hamiltonian reads

$$H[\phi]=\frac{1}{2}\int\phi(\mathbf{r})v^{-1}(\mathbf{r},\mathbf{r}')\phi(\mathbf{r}')\,\mathrm{d}\mathbf{r}\,\mathrm{d}\mathbf{r}'+\mathrm{i}\int\rho_0(\mathbf{r})\phi(\mathbf{r})\,\mathrm{d}\mathbf{r} \quad (18)$$
$$-\frac{\Lambda_c}{\beta}\int\mathrm{e}^{-\mathrm{i}\beta qe_0\phi(\mathbf{r})}\Omega(\mathbf{r})\,\mathrm{d}\mathbf{r}-\frac{\Lambda_+}{\beta}\int\mathrm{e}^{-\mathrm{i}\beta e_0\phi(\mathbf{r})}\,\mathrm{d}\mathbf{r}-\frac{\Lambda_-}{\beta}\int\mathrm{e}^{\mathrm{i}\beta e_0\phi(\mathbf{r})}\,\mathrm{d}\mathbf{r},$$

and Λ_c and $\Lambda_\pm$ represent the fugacities of polyvalent counterions and salt ions and $v^{-1}(\mathbf{r},\mathbf{r}')=-\varepsilon\varepsilon_0\nabla^2\delta(\mathbf{r}-\mathbf{r}')$ is the inverse Coulomb kernel. The special case of counterions-only system, as analyzed in the previous section, is recovered by setting $\Lambda_\pm=0$.

We shall assume that salt ions are in equilibrium with a bulk reservoir containing equal concentration n_b of both positive and negative ions, which implies $\Lambda_+=\Lambda_-\equiv n_b$. One can thus introduce the Debye-Hückel (DH) screening parameter κ (inverse "screening length") as $\kappa^2=8\pi\ell_{\rm B}n_b$. The polyvalent counterions shall be treated here within the canonical ensemble [d], i.e., their number in the slit is assumed to be fixed and equal to N. The number of counterions may be expressed via the dimensionless parameter

$$\eta=Nq/(2\sigma_{\rm s}S), \quad (19)$$

[c] We may refer to the q-valency (polyvalent) counterions simply as "counterions".
[d] see Ref.[41] for a grand-canonical description of polyvalent counterions.

where S is the area of the interacting surfaces. The case $\eta = 0$ represents a system with salt only, and $\eta = 1$ is the case where the total charge due to counterions exactly compensates the surface charge. Note that η can take any non-negative value when salt ions are present. This is because salt ions turn the long-range Coulomb potential into a short-range DH potential (see below) and can thus ensure the electroneutrality condition themselves.

6.2. *Dressed counterions*

Assuming that the system is highly asymmetric $q \gg 1$, one can formulate an approximate theory in order to evaluate the partition function (17) analytically by acknowledging the fact that the polyvalent counterions are strongly coupled while the simple salt ions are weakly coupled to the fluctuating electrostatic fields. This leads to a mixed WC-SC evaluation of the partition function.[41]

The salt terms (the last two terms) in Eq. (18) can be combined into $\cos \beta e_0 \phi(\mathbf{r})$ and in a highly asymmetric system this can be expanded up to the quadratic order in the fluctuating potential. Thus up to an irrelevant constant we remain with an effective field Hamiltonian of the form

$$H_{\text{eff}}[\phi] = \frac{1}{2} \int \phi(\mathbf{r}) v_{\text{DH}}^{-1}(\mathbf{r}, \mathbf{r}') \phi(\mathbf{r}') \, \mathrm{d}\mathbf{r} \, \mathrm{d}\mathbf{r}' + \mathrm{i} \int \rho_0(\mathbf{r}) \phi(\mathbf{r}) \, \mathrm{d}\mathbf{r} - \frac{\Lambda_c}{\beta} \int \mathrm{e}^{-\mathrm{i}\beta q e_0 \phi(\mathbf{r})} \Omega(\mathbf{r}) \, \mathrm{d}\mathbf{r}. \tag{20}$$

This procedure therefore yields an effective Hamiltonian for a "counterions-only" system but with the proviso that the inverse Coulomb kernel is replaced by the standard inverse DH kernel

$$v_{\text{DH}}^{-1}(\mathbf{r}, \mathbf{r}') = -\varepsilon\varepsilon_0(\nabla^2 - \kappa^2)\delta(\mathbf{r} - \mathbf{r}'), \quad \text{with} \quad v_{\text{DH}}(\mathbf{r}, \mathbf{r}') = \frac{\mathrm{e}^{-\kappa|\mathbf{r}-\mathbf{r}'|}}{4\pi\varepsilon\varepsilon_0|\mathbf{r} - \mathbf{r}'|}. \tag{21}$$

We have thus effectively integrated out the salt degrees of freedom leading to a renormalized interaction potential between all the remaining charge species of the screened DH form. One can thus drop any reference to explicit salt ions and infer the thermodynamic properties of the original system by analyzing it as a system composed of *dressed counterions* and fixed external charges interacting via a screened DH pair potential. In the SC limit for the polyvalent counterions we term this approximation scheme as the *SC dressed counterion theory*. Our SC analysis thus proceeds in the same way as for the counterions-only systems[13] except that the interactions between the charges are now of a dressed form.

We note that any Bjerrum pairing[53,60] or even electrostatic collapse of the salt or formation of salt-counterion complexes[61] is beyond the framework developed here.

6.3. *WC dressed counterion theory*

We again focus on a system composed of two plane-parallel surfaces defined via Eq. (16). In the WC limit (for both the counterions as well as the salt ions), the functional integral derived in the previous section is dominated by the contribution from the saddle-point solution $\phi_{\rm SP}$. This subsequently leads to the mean-field equation for the real-valued mean-field potential $\psi = {\rm i}\phi_{\rm SP}$, i.e.,

$$-\varepsilon\varepsilon_0(\nabla^2\psi - \kappa^2\psi) = \rho_0(\mathbf{r}) + qe_0\Lambda_c\Omega(\mathbf{r})\,{\rm e}^{-\beta qe_0\psi}, \tag{22}$$

which, in rescaled units $w = \beta qe_0\psi$ and by virtue of the lateral symmetry for planar surfaces $w = w(z)$, may be written as

$$w'' = \kappa^2 w - C\,{\rm e}^{-w} \qquad |z| < D/2. \tag{23}$$

The constant C can be evaluated when one stipulates the fixed amount of counterions. Outside the slit $|z| > D/2$, the mean-field equation has the standard DH form $w'' = \kappa^2 w$, which yields $w(z) = w_0 \exp(\pm\kappa z)$.

The interaction pressure, P, between the bounding surfaces is given by the difference of the ion concentrations at the mid-plane ($z = 0$), where the mean electric field vanishes, and the bulk concentration, i.e., $\beta P = n_+(0) + n_-(0) + n_c(0) - 2n_b$, which leads to the dimensionless expression

$$\frac{\beta P(D)}{2\pi\ell_{\rm B}\sigma_{\rm s}^2} = \frac{1}{4}(\kappa\mu)^2\, w^2(0) + \frac{1}{2}C\,{\rm e}^{-w(0)}. \tag{24}$$

As evident from the above equation, the pressure can never be negative and the effective interaction is thus *always repulsive* within this type of mean-field approach.[62] The canonical mean-field equation (23) can be solved numerically and the results can be used to evaluate the pressure (24) as a function of the inter-surface separation (Fig. 4(a), dashed line).

6.4. *SC dressed counterion theory*

The analysis of the dressed counterions system in the SC limit is very similar to the traditional SC approach in the case of counterions only.[13] We proceed by expanding the grand-canonical partition function associated with the dressed counterion approximation, Eq. (20), to the first order in counterion

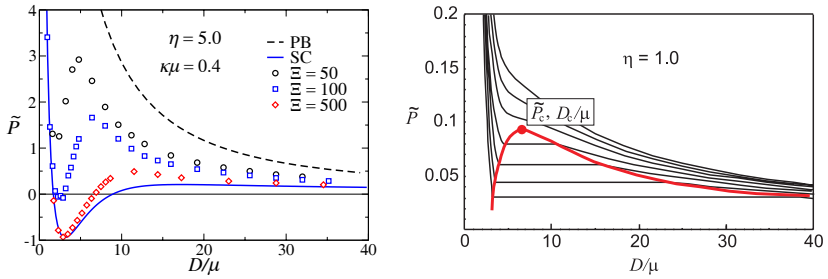

(a) (b)

Fig. 4. a) Rescaled interaction pressure $\tilde{P} \equiv \beta P(D)/(2\pi\ell_{\rm B}\sigma_{\rm s}^2)$ between two like-charged surfaces as a function of the rescaled inter-surface distance. b) Van der Waals type iso-inverse screening length curves are shown along with the corresponding Maxwell construction. The inverse screening length is varied in the range from $\kappa\mu = 0.4$ to $\kappa\mu = 0.56$ in intervals of 0.027 (from bottom to top).

fugacity, Λ_c. We then perform an inverse Legendre transformation[e] in order to obtain the canonical SC free energy.[13,46] We thus find

$$\mathcal{F}_N = U_0 - Nk_{\rm B}T \ln \int {\rm e}^{-\beta u(\mathbf{r})}\, {\rm d}\mathbf{r}, \tag{25}$$

where the first term is the screened interaction energy of fixed charges

$$U_0 = \frac{1}{2}\int \rho_0(\mathbf{r}) v_{\rm DH}(\mathbf{r},\mathbf{r}')\rho_0(\mathbf{r}')\, {\rm d}\mathbf{r}\, {\rm d}\mathbf{r}', \tag{26}$$

and the term in the exponent is the single-particle interaction energy of the dressed counterions with fixed macroion charges

$$u(\mathbf{r}) = qe_0 \int \rho_0(\mathbf{r}') v_{\rm DH}(\mathbf{r},\mathbf{r}')\, {\rm d}\mathbf{r}'. \tag{27}$$

The SC attraction between like-charged macroions stems from the second term in Eq. (25), which contains the counterion-induced effects.[13,15,16,46]

For the planar system under consideration (Eq. (16)), the above quantities may be evaluated explicitly[41] and we find the SC free energy as

$$\beta\mathcal{F}_N/N = \frac{1}{2\kappa\mu\eta}\, {\rm e}^{-\kappa D} - \ln\, I(D), \tag{28}$$

[e]This is achieved by mapping the fugacity to the number of counterions, N, via the relation $\Lambda_c \partial \ln \mathcal{Z}/\partial\Lambda_c = N$.

where we have introduced

$$I(D) = \int_0^{D/2} \exp\Big(\frac{2}{\kappa\mu}\,\mathrm{e}^{-\kappa D/2}\cosh\,\kappa z\Big)\,\mathrm{d}z. \tag{29}$$

The first term in Eq. (28) corresponds to the usual salt-mediated repulsive DH interaction between the two surfaces, and the second one is the contribution of counterions, which is proportional to η, Eq. (19), on the single-particle SC level.

The dimensionless pressure acting between the surfaces can be obtained from the free energy via the standard thermodynamic relation $P = -\partial(\mathcal{F}_N/S)/\partial D$, thus yielding

$$\frac{\beta P(D)}{2\pi\ell_{\rm B}\sigma_{\rm s}^2} = \mathrm{e}^{-\kappa D} + 2\eta\,\frac{I'(D)}{I(D)}, \tag{30}$$

where the prime denotes the derivative with respect to the argument.

The analytical SC pressure (30) is shown in Fig. 4(a) as a function of the inter-surface distance (solid curve) along with the results from Monte-Carlo simulations[41] (symbols) for a few different screening parameters. We also show in the figure the WC pressure from Eq. (24) (dashed curve). First note that the simulation results are bracketed by the two limiting analytical theories of WC and SC within the dressed counterion scheme and thus agree with the general feature obtained before[13–16] that the WC and SC limits in fact establish the upper and lower bounds for the interaction pressure between charged surfaces.

For both small and large separations the interaction pressure becomes positive (repulsive), whereas for a sufficiently large coupling parameter,[41] an effective inter-surface attraction can emerge at intermediate separations between the walls. For $\kappa D \ll 1$, the SC pressure reduces to

$$\frac{\beta P(D)}{2\pi\ell_{\rm B}\sigma_{\rm s}^2} \simeq \frac{2\mu\eta}{D} + (1-2\eta), \tag{31}$$

which to the leading order corresponds to the ideal-gas osmotic pressure of counterions squeezed between the two surfaces. For $\kappa D \gg 1$, the pressure behaves as

$$\frac{\beta P(D)}{2\pi\ell_{\rm B}\sigma_{\rm s}^2} \simeq \frac{2\mu\eta}{D} - \frac{4\eta}{(\kappa D)^2}, \tag{32}$$

which indicates that at large separations the counterions again behave as an ideal gas on the leading order as all electrostatic interactions are effectively screened out and hence only the repulsive osmotic contribution remains.

The interaction pressure in the canonical ensemble thus always possesses repulsive branches at small and large separations and can show non-monotonic behavior in between. In fact, for certain values of the parameters the interaction pressure shows a van der Waals-like loop which could suggest a coexistence regime between two different "phases". This loop is obtained for certain iso-ionic strength curves. From a thermodynamic perspective one thus has a coexistence between a dense phase, identified with a small inter-surface separation, at equilibrium with an expanded phase with a larger inter-surface separation. Such van der Waals-like coexistence between interacting charged surfaces has been seen in other contexts before[63] and can be demonstrated by means of a Maxwell construction analysis as shown in Fig. 4(b).

In an experiment such as osmotic stress experiments and surface force experiments[8] one can only probe stable equilibrium states of the system implying interaction pressure vs. separation curves that are in agreement with the appropriate Maxwell construction. The binodal or the coexistence curve, which delimits the region in the pressure-separation plots where a Maxwell construction is feasible (red curve in Fig. 4(b)), ends at a critical point corresponding to a critical amount of salt above which the interaction pressure remains purely repulsive. For the case with $\eta = 1$, we find the critical point as ($\tilde{P}_c = 0.092$, $D_c/\mu = 6.14$, $\kappa_c\mu = 0.546$).

It is interesting to note that this type of interaction pressure equilibria corresponding to abrupt transitions from one equilibrium separation to a different one have been observed in experiments with strongly charged macromolecules in the presence of polyvalent counterions and univalent salt. A typical example would be the osmotic stress experiments on DNA in the presence of trivalent CoHex counterions and 0.25M NaCl salt, that show abrupt transitions in osmotic pressure for intermediate $CoHex^{3+}$ concentrations from one repulsive osmotic pressure branch to another one.[57] Similar features are discerned even for a divalent counterion Mn^{2+} at various concentrations or temperatures.[58]

The agreement between the SC dressed counterion theory and simulations becomes better as the coupling parameter Ξ becomes larger. The agreement is also better for a smaller fraction of counterions, η, in the slit. Using a similar argument as in the counterions-only case in Section 5.2,[13–16] we find that the theory is expected to hold at small separations given by $D/\mu \ll \sqrt{\Xi/\eta}$. Thus, for $\eta < 1$ (i.e., when the amount of the bare charge due counterions is less than the bare fixed charge on the macroions), the SC dressed counterion theory is expected to hold in a wider range of

separations as compared with the original counterions-only SC theory.[13] At very large separations, where most of the electrostatics is screened out, the interaction between counterions becomes negligible and the SC theory of dressed counterions retains its validity again. This result is a consequence of the dressed counterion theory and is not obtained in the standard SC theory with counterions only. Thus, the SC dressed counterion theory captures the physics both at large and small separations but would require improvements at intermediate separations.

It should be noted that the validity of the DH-type linearization that we have used to derive the dressed interaction potentials is also limited by stipulating that the dimensionless DH potential itself is always small enough. This leads to the condition that $\kappa \gg 2\pi\ell_{\rm B}\sigma_{\rm s}$, or $\kappa\mu \gg 1/q$, which turns out to cover a whole range of realistic parameter values.[41]

7. Counterions between Randomly Charged Surfaces

The assumption of homogeneity of surface charges is in general quite severe and there are well known cases where this assumption is not realistic at all. Random polyelectrolytes and polyampholytes present one such case.[64–66] There the sequence of charges can be distributed along the polymer backbone in a disordered manner where the disorder distribution may be of a *quenched* type. The Coulomb (self-)interactions of such polyelectrolytes are distinct and different from homogeneously charged polymers.

A case even closer to the present line of reasoning are investigations of interactions between solid surfaces in the presence of charged surfactants. The aggregation of surfactants on crystalline hydrophobic substrates in aqueous solutions can sometimes show structures consistent with highly inhomogeneous and disordered surface charge distributions.[67] Similar interfacial structures are seen for interacting hydrophilic mica surfaces in the presence of cetyl-trimethyl-amonium bromide (CTAB) or other surfactant-coated surfaces.[68] The surfaces appear to be covered by a mosaic of positively and negatively charged regions and experience a strong, *long-ranged attraction*, which is comparable in magnitude to that between hydrophobic surfaces, and is orders of magnitude larger than the expected Lifshitz-van der Waals forces.[68] The patterning of interacting surfaces described above is highly disordered, depends on the method of preparation and has basic implications also for the forces that act between other types of hydrophilic surfaces with mixed charges.

It thus seem appropriate to investigate the effect of quenched disordered charge distribution on the interactions between macroions in ionic solutions.[f] As a particular case, we shall again focus on the effective interaction between two randomly charged planar surfaces across a one-component Coulomb fluid.[42]

7.1. *General formalism: The replica method*

The partition function of a Coulomb fluid in the presence of an external fixed charge distribution $\rho_0(\mathbf{r})$, can be again written in the form of a functional integral over the fluctuating electrostatic field $\phi(\mathbf{r})$ as given in Eq. (17). However, the fixed charges are now assumed to be randomly distributed on macromolecular surfaces. Thus $\rho_0(\mathbf{r})$ is represented by a probability distribution, which is assumed to be Gaussian with no spatial correlations, i.e.

$$\mathcal{P}[\rho_0(\mathbf{r})] = \text{const.} \times \mathrm{e}^{-\frac{1}{2}\int \mathrm{d}\mathbf{r}\; g^{-1}(\mathbf{r})\,(\rho_0(\mathbf{r})-\bar{\rho}_0(\mathbf{r}))^2}, \tag{33}$$

where $\bar{\rho}_0(\mathbf{r})$ is the mean value and $g(\mathbf{r})$ the width or variance of the charge disorder distribution. For clarity, we shall also focus on the counterions-only case by setting $\Lambda_\pm = 0$ in Eq. (18).

The average over quenched charge disorder is now obtained by applying the standard Edwards-Anderson replica ansatz[69,70] in the form

$$\mathcal{F} = -k_\mathrm{B}T\,\overline{\ln \mathcal{Z}} = -k_\mathrm{B}T\,\lim_{n\to 0}\frac{\overline{\mathcal{Z}^n}-1}{n}, \tag{34}$$

where the disorder average is defined as $\overline{(\dots)} = \int \mathcal{D}\rho_0\,(\cdots)\,\mathcal{P}[\rho_0(\mathbf{r})]$.

The Gaussian integrals involved in Eq. (34) can be evaluated straightforwardly and the final form of the replicated partition function follows as[42]

$$\overline{\mathcal{Z}^n} = \int \left[\prod_{a=1}^{n}\mathcal{D}\phi_a\right] \mathrm{e}^{-\beta\mathcal{S}[\phi_a(\mathbf{r})]}, \tag{35}$$

with

$$\mathcal{S}[\phi_a(\mathbf{r})] = \frac{1}{2}\sum_{a,b}\int \phi_a(\mathbf{r})\mathcal{D}_{ab}(\mathbf{r},\mathbf{r}')\phi_b(\mathbf{r})\,\mathrm{d}\mathbf{r}\,\mathrm{d}\mathbf{r}' + \mathrm{i}\int \bar{\rho}_0(\mathbf{r})\sum_a \phi_a(\mathbf{r})\,\mathrm{d}\mathbf{r} - \frac{\Lambda_c}{\beta}\int \Omega(\mathbf{r})\sum_a \mathrm{e}^{-\mathrm{i}\beta q e_0\phi_a(\mathbf{r})}\,\mathrm{d}\mathbf{r}, \tag{36}$$

[f]See Refs.[44,45] for an analysis of the effects due to annealed and partially annealed charge disorder.

where $a, b = 1, \ldots, n$ are the replica indices and

$$\mathcal{D}_{ab}(\mathbf{r}, \mathbf{r}') = u^{-1}(\mathbf{r}, \mathbf{r}')\delta_{ab} + \beta g(\mathbf{r})\delta(\mathbf{r} - \mathbf{r}'). \tag{37}$$

The expression (35) together with Eq. (34) represents the starting formulation for the free energy in the presence of quenched charge disorder. This free energy can only be evaluated approximately. Thus, in order to proceed we shall combine the methods developed for the one-component (counterions-only) Coulomb fluid without disorder[13] and modify them in order to incorporate appropriately the disorder effects. We shall start with the WC limit giving rise to the corresponding mean-field theory and then proceed to the SC limit.

7.2. *Disorder effects in the WC regime*

In the WC limit $\Xi \to 0$, one may proceed by employing a saddle-point analysis of the functional integral (35), just as in the case with no disorder in Section 6.3. It is easy to show that the real-valued mean-field replica potential ψ_a is governed by the following equation,

$$-\varepsilon\varepsilon_0\nabla^2\psi_a(\mathbf{r}) + \beta g(\mathbf{r})\sum_{b=1}^{n}\psi_b(\mathbf{r}) = \bar{\rho}_0(\mathbf{r}) + qe_0\Lambda_c\Omega(\mathbf{r})\,\mathrm{e}^{-\beta qe_0\psi_a}. \tag{38}$$

In the replica formulation we have to take the limit $n \to 0$, which furthermore implies that $\lim_{n\to 0}\sum_b \psi_b(\mathbf{r}) \to 0$. It is thus evident that in the limit $n \to 0$, the contributions from the disorder vanish and, because the index a becomes irrelevant, one recovers the standard PB equation (7). Therefore, the quenched charge disorder effects completely vanish in the WC limit.[42,71]

The above result is a consequence of the mean-field approximation and holds in the limit $\Xi \to 0$ even if the system is generalized to contain additional ionic species or dielectric discontinuities at the bounding surfaces. The quenched charge disorder however turns out to play a significant role in dielectrically inhomogeneous systems when electrostatic field fluctuations are taken into account. It can be shown to lead to an additional attractive or repulsive contribution to the total free energy (depending on the dielectric mismatch and the salt screening in the system) even when the surfaces are assumed to be *net-neutral*.[43,44]

7.3. *Disorder effects in the SC regime*

The partition function (35) can be calculated in the SC limit via a virial expansion up to the first nontrivial leading order in powers of the fugacity

as noted before. The canonical SC free energy of the system then follows from Eq. (34) by using a standard Legendre transform[42] as

$$\mathcal{F}_N = \frac{1}{2}\int \bar{\rho}_0(\mathbf{r})v(\mathbf{r},\mathbf{r}')\bar{\rho}_0(\mathbf{r}')\,\mathrm{d}\mathbf{r}\,\mathrm{d}\mathbf{r}' + \frac{1}{2}\mathrm{Tr}\, g(\mathbf{r})v(\mathbf{r},\mathbf{r}') - Nk_\mathrm{B}T\,\ln\int \Omega(\mathbf{R})\,\mathrm{e}^{-\beta u(\mathbf{R})}\,\mathrm{d}\mathbf{R}. \tag{39}$$

The first term in Eq. (39) is nothing but the direct Coulomb interaction between the mean charge densities $\bar{\rho}_0(\mathbf{r})$ of the fixed charged surfaces (macroions). The second term is an additive contribution from the charge disorder, which becomes important only in dielectrically inhomogeneous systems[43,44] and will be irrelevant in the present study. The third term, however, embodies the disorder effects on the SC level in the presence of a Coulomb fluid. It depends on the single-particle interaction potential

$$u(\mathbf{R}) = qe_0\int v(\mathbf{r}',\mathbf{R})\bar{\rho}_0(\mathbf{r}')\,\mathrm{d}\mathbf{r}' - \frac{\beta}{2}(qe_0)^2\int g(\mathbf{r}')v^2(\mathbf{r}',\mathbf{R})\,\mathrm{d}\mathbf{r}', \tag{40}$$

where the second term comes from the disorder variance $g(\mathbf{r})$ and exhibits a non-trivial dependence on the Coulomb kernel $v(\mathbf{r},\mathbf{r}') = 1/(4\pi\varepsilon\varepsilon_0|\mathbf{r}-\mathbf{r}'|)$.

Assuming again that our system is composed of two planar surfaces located at $z = \pm D/2$ with statistically identical random charge distributions, we write the mean density and variance of the disordered surface charge as

$$\bar{\rho}_0(\mathbf{r}) = -\sigma_\mathrm{s}e_0\big[\delta(z-D/2)+\delta(z+D/2)\big],\;\; g(\mathbf{r}) = ge_0^2\big[\delta(z-D/2)+\delta(z+D/2)\big]. \tag{41}$$

The electroneutrality again stipulates that $2\sigma_\mathrm{s}S = Nq$. The geometry function $\Omega(\mathbf{R})$ is the same as before. All the terms in the expression for the free energy, Eq. (39), can be computed explicitly. At the end we obtain a surprisingly simple expression

$$\frac{\beta\mathcal{F}_N}{N} = \frac{D}{2\mu} + (\chi-1)\,\ln\,D. \tag{42}$$

Here we have introduced the dimensionless *disorder coupling parameter*

$$\chi = 2\pi q^2\ell_\mathrm{B}^2 g, \tag{43}$$

which is very similar to the electrostatic coupling parameter, Ξ, in Eq. (4), except that it is defined based on the disorder variance g and scales with the counterion valency as q^2 instead of q^3. The free energy (42) is plotted in Fig. 5(a) for different values of the disorder coupling parameter. Note that the disorder leads to a long-range attractive contribution, which is *additive* in the SC free energy and has a logarithmic dependence on the

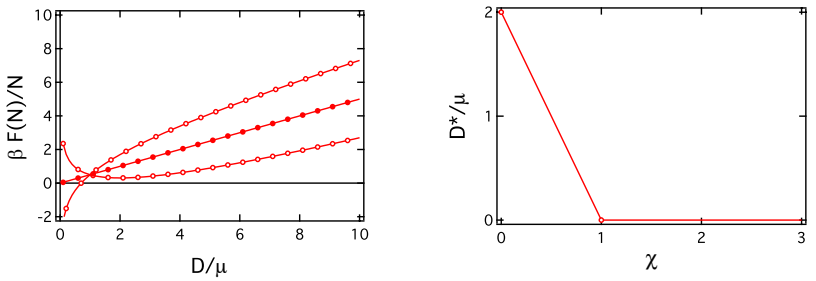

(a) (b)

Fig. 5. Left: Rescaled SC free energy, Eq. (42), of two charged walls bearing quenched charge disorder as a function of the rescaled inter-surface distance D/μ for $\chi = 0, 1$ and 2 (bottom line, middle line, top line). Right: Rescaled equilibrium distance D^*/μ as a function of the disorder coupling parameter χ.

separation, i.e., $\chi \ln D$. It thus appears that the quenched charge disorder and the counterions confinement entropy, i.e., the $-\ln D$ term in Eq. (42), in some sense counteract one another.

Evaluating the interaction pressure from the free energy, Eq. (42), we find $P(D) = P_{\rm SC}(D) + P_{\rm disorder}(D)$, where the first term is the standard SC pressure,[13] Eq. (13), and the second term is the additive contribution from the disorder

$$\frac{\beta P_{\rm disorder}(D)}{2\pi\ell_{\rm B}\sigma_{\rm s}^2} = -\chi\left(\frac{2\mu}{D}\right). \tag{44}$$

We can then derive the equilibrium distance D^* between the two surfaces, corresponding to zero interaction pressure, as

$$D^* = 2\,(1-\chi)\,\mu. \tag{45}$$

In the undisordered case, $\chi = 0$, this reduces to the known result $D^* = 2\mu$,[13] which corresponds to a stable bound state for the two surfaces at a separation equal to twice the GC length. However, as χ is increased, the equilibrium separation decreases and vanishes at the critical value $\chi_c = 1$ and remains at zero thereafter. This behavior has all the features of a second-order, quenched-disorder-induced *collapse transition* with an unusual value of the critical exponent (see Fig. 5(b)). Note also that for $\chi = 1$ the interaction pressure between the surfaces is obviously constant in the whole range of separations D right down to zero as the counterions confinement entropy is completely wiped out by the charge disorder contribution.

8. Lessons

The two limiting laws, i.e., the WC and the SC limits for Coulomb fluids that we explored above, are valid in disjoint regions of the parameter space. While the WC limit is valid for sufficiently small macroion surface charge densities, low counterion valencies, high medium dielectric constant and/or high temperatures, the SC limit becomes valid for respectively opposite parameter values. The two together bracket the region of all possible behaviors of Coulomb fluids confined between charged boundaries, a view that was completely corroborated by extensive simulation studies.

The parameter space in between these limiting values can be analyzed by approximate methods[72–74] but is most often accessible solely via computer simulations.[13–16,41,46–49,51,72,74–76] Exact solutions for the whole range of coupling parameters are unfortunately available only in one dimension.[77] The *WC-SC paradigm* has been tested extensively[13–16,41,46–49,51,72–74,77] and fits computer simulations quantitatively correctly in the respective regimes of validity, thus providing a unifying conceptual framework of the behavior of Coulomb fluids.

Though we have shown that in the important limit of SC the much cherished and widespread PB approach does not work, formally its applicability can be systematically extended by perturbative corrections in the local potential fluctuations and correlations[12–14,51,54,78–81] along the lines of the standard approach used in the mean-field context.[82] This kind of fix is nevertheless severely limited since the perturbative expansion is only weakly convergent[13–16] and higher-order corrections beyond the first-loop Gaussian term are very complicated and difficult to carry through.[80,81] Such perturbative corrections offer in effect only a relatively insignificant improvement over the PB approximation[13–16,51] and can not predict phenomena such as like-charge attraction.[75]

The emerging world of Coulomb interactions reviewed above is indeed fascinating. While the counterion-mediated electrostatic interactions between equally charged surfaces are always repulsive on the WC level, the SC regime offers a much richer framework with plethora of new phenomena. Interactions between equally charged macromolecular surfaces can be attractive for strongly coupled counterions, or non-monotonic–showing repulsion at small and large as well as attraction at intermediate separations–for strongly coupled counterions in the presence of weakly coupled simple salt. While charge disorder on macromolecular surfaces has no effect on the WC level, it can quite unexpectedly lead to strong electrostatic

attractions between randomly charged surfaces on the SC level. In view of these developments, the commonly held pop culture wisdom that likes repel and opposites attract should thus be *substantially amended!*

Acknowledgment

Rudolf Podgornik would like to acknowledge the financial support by the Slovenian Research Agency under contract Nr. P1-0055 (Biophysics of Polymers, Membranes, Gels, Colloids and Cells) and under contract Nr. J1-0908 (Dispersion force nanoactuators). Matej Kanduč would like to acknowledge the financial support by the Slovenian Research Agency under the young researcher grant. Ali Naji is supported by a Newton International Fellowship from the Royal Society, the Royal Academy of Engineering, and the British Academy.

References

1. E. T. Whittaker, *A History of the Theories of Aether and Electricity: The Classical Theories, the Modern Theories 1900-1926* (Two Volumes Bound As One, Dover Classics Edition, 1990).
2. R. French et al., Rev. Mod. Phys. **82**, 1887 (2010).
3. G. Gouy, J. Phys. (Paris) **9**, 457 (1910).
4. D.L. Chapman, Phil. Mag. **25**, 475 (1913).
5. P. Debye, E. Hückel, Physik. Z. **24**, 185 (1923).
6. B.V. Derjaguin, L. Landau, Acta Physicochim. USSR **14**, 633 (1941).
7. E.J. Verwey, J.T.G. Overbeek, *Theory of the Stability of Lyophobic Colloids* (Elsevier, Amsterdam, 1948).
8. J. Israelachvili, *Intermolecular and Surface Forces* (Academic Press, London, 1991).
9. R.J. Hunter, *Foundations of Colloidal Science* (Clarendon, Oxford, first edition 1987, second edition 2001).
10. V.A. Parsegian, *Van der Waals Forces* (Cambridge University Press, Cambridge, 2005).
11. S. F. Edwards, A. Lenard, J. Math. Phys. **3**, 778 (1962).
12. R. Podgornik, B. Žekš, J. Chem. Soc., Faraday Trans 2 **5**, 611 (1988); R. Podgornik, J. Phys. A **23**, 275 (1990); J. Chem. Phys. **91**, 5840 (1989).
13. R.R. Netz, Eur. Phys. J. E **5**, 557 (2001).
14. A.G. Moreira, R.R. Netz, Europhys. Lett. **52**, 705 (2000); Phys. Rev. Lett **87**, 078301 (2001); Eur. Phys. J. E **8**, 33 (2002).
15. H. Boroudjerdi, Y.-W. Kim, A. Naji, R.R. Netz , X. Schlagberger, A. Serr, Physics Reports (2005).
16. A. Naji, S. Jungblut, A.G. Moreira, R.R. Netz, Physica A **352**, 131 (2005).
17. I. Rouzina, V.A. Bloomfield, J. Phys. Chem. **100**, 9977 (1996).

18. A.Yu. Grosberg, T.T. Nguyen, B.I. Shklovskii, Rev. Mod. Phys. **74**, 329 (2002).
19. Y. Levin, Rep. Prog. Phys. **65**, 1577 (2002).
20. C. Holm, P. Kekicheff, R. Podgornik (Eds.), *Electrostatic Effects in Soft Matter and Biophysics*, Kluwer Academic, Dordrecht, 2001.
21. W. C. K. Poon, D. Andelman (Eds.), *Soft condensed matter physics in molecular and cell biology*, Taylor & Francis, New York, London, 2006.
22. B. Alberts, A. Johnson, J. Lewis, M. Raff, K. Roberts, P. Walter, *Molecular Biology of the Cell* (Garland Science, New York, 2002).
23. D.H. Napper, *Polymeric Stabilization of Colloidal Dispersions* (Academic Press, London, 1983).
24. P. Pincus, Macromolecules **24**, 2912 (1991).
25. H. Dautzenberg, W. Jaeger, B.P.J. Kötz, C. Seidel, D. Stscherbina, *Polyelectrolytes: Formation, characterization and application* (Hanser Publishers, New York, 1994).
26. F. Oosawa, *Polyelectrolytes* (Marcel Dekker, New York, 1971).
27. K.K. Kunze, R.R. Netz, Phys. Rev. Lett. **85**, 4389 (2000).
28. H. Boroudjerdi, R.R. Netz, Europhys. Lett. **64**, 413 (2003); J. Phys.: Condens. Matter **17**, S1137 (2005); Europhys. Lett. **71**, 1022 (2005).
29. J.O. Rädler, I. Koltover, T. Salditt, C.R. Safinya, Science **275**, 810 (1997).
30. J.O. Rädler, I. Koltover, A. Jamieson, T. Salditt, C.R. Safinya, Langmuir **14**, 4272 (1998).
31. I. Koltover, T. Salditt, J.O. Rädler, C.R. Safinya, Science **281**, 78 (1998).
32. R.G. Crystal, Science **270**, 404 (1995).
33. W.M. Gelbart, R.F. Bruinsma, P.A. Pincus, V.A. Parsegian, Physics Today (September 2000), pp. 38-44.
34. V.A. Bloomfield, Biopolymers **31**, 1471 (1991); Curr. Opin. Struct. Biol. **6**, 334 (1996).
35. O. Lambert, L. Plançon, J.L. Rigaud, L. Letellier, Mol. Microbiol. **30**, 761 (1998).
36. J.X. Tang, S. Wong, P.T. Tran, P.A. Janmey, Ber. Bunsenges. Phys. Chem. **100**, 796 (1996).
37. J.X. Tang, T. Ito, T. Tao, P. Traub, P.A. Janmey, Biochemistry **36**, 12600 (1997).
38. D. J. Needleman, M. A. Ojeda-Lopez, U. Raviv, H. P. Miller, L. Wilson, C. R. Safinya, Proc. Natl. Acad. Sci. USA **101**, 16099 (2004).
39. D. Ben-Yaakov, D. Andelman, D. Harries, R. Podgornik, J. Phys.: Condens. Matter **21** 424106 (2009).
40. Y. Burak, D. Andelman, Phys. Rev. E **62**, 5296 (2000); J. Chem. Phys. **114**, 3271 (2001)
41. M. Kanduc, A. Naji, J. Forsman, R. Podgornik, J. Chem. Phys. **132**, 124701 (2010).
42. A. Naji, R. Podgornik, Phys. Rev. E **72**, 041402 (2005).
43. R. Podgornik, A. Naji, Europhys. Lett. **74**, 712 (2006).
44. A. Naji, D.S. Dean, J. Sarabadani, R. Horgan, R. Podgornik, Phys. Rev. Lett. **104**, 060601 (2010).

45. Y.Sh. Mamasakhlisov, A. Naji, R. Podgornik, J. Stat. Phys. **133**, 659 (2008).
46. A. Naji, R. R. Netz, Eur. Phys. J. E **13**, 43 (2004); A. Naji, A. Arnold, C. Holm, R. R. Netz, Europhys. Lett. **67**, 130 (2004).
47. A. Naji, R. R. Netz, Phys. Rev. Lett. **95**, 185703 (2005); Phys. Rev. E **73**, 056105 (2006).
48. M. Kanduč, J. Dobnikar, R. Podgornik, Soft Matter **5**, 868 (2009); M. Kanduc, A. Naji, R. Podgornik, J. Chem. Phys. **132**, 224703 (2010).
49. Y.S. Jho, M. Kanduč, A. Naji, R. Podgornik, M.W. Kim, P.A. Pincus, Phys. Rev. Lett. **101**, 188101 (2008).
50. M. Kanduč, R. Podgornik, Eur. Phys. J. E **23**, 265 (2007).
51. M. Kanduč, M. Trulsson, A. Naji, Y. Burak, J. Forsman, R. Podgornik, Phys. Rev. E **78**, 061105 (2008).
52. M. Kanduč, A. Naji, Y. S. Jho, P. A. Pincus, R. Podgornik, J. Phys.: Condens. Matter **21**, 424103 (2009).
53. N. Bjerrum, Kgl. Danske Videnskab. Selskab. Mat.-fys. Medd. **7**, 1 (1926).
54. R.R. Netz, H. Orland, Eur. Phys. J. E **1**, 203 (2000).
55. H. Wennerström, B. Jönsson, P. Linse, J. Chem. Phys. **76**, 4665 (1982).
56. M. Baus, J. Hansen, Phys. Rep. **59**, 1 (1980).
57. D.C. Rau, V. A. Parsegian, Biophys J **61**, 246 (1992).
58. D.C. Rau, V. A. Parsegian, Biophys J **61**, 260 (1992).
59. O. Punkkinen, A. Naji, R. Podgornik, I. Vattulainen, P.-L. Hansen, Europhys. Lett. **82**, 48001 (2008).
60. J. Zwanikken, R. van Roij, J. Phys.: Condens. Matter **21**, 424102 (2009).
61. M. E. Fisher, Y. Levin, Phys. Rev. Lett. **71**, 3826 (1993).
62. J.C. Neu, Phys. Rev. Lett. **82**, 1072 (1999); J.E. Sader, D.Y.C. Chan, J. Colloid Interface Sci. **213**, 268 (1999); Langmuir **16**, 324 (2000); E. Trizac, J.-L. Raimbault, Phys. Rev. E **60**, 6530 (1999); E. Trizac, Phys. Rev. E **62**, R1465 (2000).
63. D. Harries, R. Podgornik, V.A. Parsegian, E. Mar-Or, D. Andelman, J. Chem. Phys. **124**, 224702 (2006).
64. I. Borukhov, D. Andelman, H. Orland, Eur. Phys. J. B **5**, 869 (1998).
65. Y. Kantor, M. Kardar, Europhys. Lett. **28**, 169 (1994); **14**, 421 (1991).
66. Y. Kantor, M. Kardar, D. Ertas, Physica A **249**, 301 (1998).
67. S. Manne, J.P. Cleveland, H.E. Gaub, G.D. Stucky, P.K. Hansma, Langmuir **10**, 4409 (1994); S. Manne, H.E. Gaub, Science **270**, 1480 (1995).
68. E.E. Meyer, Q. Lin, T. Hassenkam, E. Oroudjev, J.N. Israelachvili, Proc. Natl. Acad. Sci. USA **102**, 6839 (2005); S. Perkin, N. Kampf, J. Klein, Phys. Rev. Lett. **96**, 038301 (2006); J. Phys. Chem. B **109**, 3832 (2005); E.E. Meyer, K.J. Rosenberg, J. Israelachvili, Proc. Natl. Acad. Sci. USA **103**, 15739 (2006).
69. J.W. Negele, H. Orland, *Quantum Many-Particle Systems* (Perseus Books Group, New York, 1998).
70. V. Dotsenko, *Introduction to the Replica Theory of Disordered Statistical Systems* (Cambridge University Press, New York, 2001).
71. C. Fleck, R.R. Netz, Europhys. Lett. **70**, 341 (2005).
72. J. Forsman, J. Phys. Chem. B **108**, 9236 (2004).

73. Y. Burak, D. Andelman, H. Orland, Phys. Rev. E **70**, 016102 (2004); C. D. Santangelo, Phys. Rev. E **73**, 041512 (2006); M. M. Hatlo, L. Lue, Soft Matter **5**, 125 (2009).
74. Y.-G. Chen, J. D. Weeks, Proc. Natl. Acad. Sci. **103**, 7560 (2006); J. M. Rodgers, C. Kaur, Y.-G. Chen, J. D. Weeks, Phys. Rev. Lett. **97**, 097801 (2006).
75. L. Guldbrand, B. Jönsson, H. Wennerström, P. Linse, J. Chem. Phys. **80**, 2221 (1984); D. Bratko, B. Jönsson, H. Wennerström, Chem. Phys. Lett. **128**, 449 (1986); J. P. Valleau, R. Ivkov, G. M. Torrie, J. Chem. Phys. **95**, 520 (1991); R. Kjellander, T. Åkesson, B. Jönsson, S. Marčelja, J. Chem. Phys. **97**, 1424 (1992).
76. M. Trulsson, B. Jönsson, T. Åkesson, J. Forsman, C. Labbez, Phys. Rev. Lett. **97**, 068302 (2006); Langmuir **23**, 11562 (2007).
77. D.S. Dean, R.R. Horgan, D. Sentenac, J. Stat. Phys. **90**, 899 (1998); D.S. Dean, R.R. Horgan, A. Naji, R. Podgornik, J. Chem. Phys. **130**, 094504 (2009).
78. P. Attard, J. Mitchell, B. W. Ninham, J. Chem. Phys. **88**, 4987 (1988).
79. B.-Y. Ha, A. J. Liu, Phys. Rev. Lett. **79**, 1289 (1997); P. A. Pincus, S.A. Safran, Europhys. Lett. **42**, 103 (1998); M. Kardar, R. Golestanian, Rev. Mod. Phys. **71**, 1233 (1999); R. R. Netz, H. Orland, Eur. Phys. J. E **1**, 203 (2000); B.-Y. Ha, Phys. Rev. E **64**, 031507 (2001); A. W. C. Lau, P. Pincus, Phys. Rev. E **66**, 041501 (2002).
80. R. Podgornik, V. A. Parsegian, Phys. Rev. Lett. **80**, 1560 (1997).
81. D. S. Dean, R. R. Horgan, J. Phys. C. **17**, 3473, (2005); Phys. Rev. E **69**, 061603 (2004); *ibid* **70**, 011101 (2004); *ibid* **68**, 061106 (2003).
82. P. Ziherl, R. Podgornik, S. Žumer, Chem. Phys. Lett. **295**, 99 (1998).